













index (e.g., c-Si and a-Si).

Figure 2(a) shows that the absorption in a c-Si layer can be enhanced by at most 20% by the presence of a silver NP (left axis in the graph), provided large ( $\geq 35$  nm) diameter NPs are used. This behavior seems in contradiction with the fact that for larger NPs the resonance shifts towards larger wavelengths, i.e. to a spectral region where silicon is less absorbing. However, this effect is counterbalanced both by the increase of the particle near-field volume in the Si and the larger absorption cross section for larger particles. Furthermore, for particle diameters larger than 30 nm the onset of a quadrupole resonance in the 700-800 nm spectral range is observed (see inset, red line). This resonance also contributes to enhanced near-field absorption in the c-Si. Overall, the absorption enhancement in c-Si is thus limited to 20%, while the average absorptance of the c-Si substrate remains below 14% (right axis in Fig. 2(a)). It must thus be concluded that embedding Ag NPs in c-Si does not provide a means to achieve strong NP-enhanced absorption of light in the c-Si.

Figure 2(b) shows that a 100% absorption enhancement can be achieved in the PF10TBT:PCBM substrate, due to the plasmonic near-field coupling. Here too, the absorption enhancement increases for larger particle diameter as a result of the increased near-field volume and larger NP absorption cross section. The average absorptance (right axis) is increased from 17% to 34% by the presence of the Ag NPs for increasing nanoparticle diameter and then levels off.

Figure 2(c) shows that by embedding a silver NP in an a-Si substrate the absorption in the semiconductor actually decreases for larger diameters. This is due to the fact that the plasmon resonance of Ag particles in a-Si occurs for wavelengths (see inset) that are larger than the bandgap wavelength of a-Si (750 nm). Thus, the strong interaction of light with the NP occurs in a spectral range where the material is only very poorly absorbing. The reduced absorption for larger diameters is due to the fact that in the simulations the total volume of a-Si decreases, as the simulation box size is fixed.

In the case of a  $\text{Fe}_2\text{O}_3$  substrate (Fig. 2(d)), the embedded plasmonic NP enhances the absorption in the semiconductor up to a factor of 24%. The average absorptance is increased from 30% to 37%. Similarly to the case of c-Si, the resonance wavelength (inset) is below the bandgap wavelength of the material (765 nm), but in a spectral region where  $\text{Fe}_2\text{O}_3$  is poorly absorbing [23, 33].

Figure 2 demonstrates that large absorption enhancements can be achieved in several semiconductors due to the plasmonic near field enhancement. However, as observed in the spectra of Fig. 1, significant optical losses occur due to Ohmic dissipation in the NPs. Figure 3 compares the fraction of the incident power that is absorbed in the semiconductor (blue), in the metal NP (red) or is not absorbed (green), as a function of particle diameter, for c-Si (a), PF10TBT:PCBM (b), a-Si (c) and  $\text{Fe}_2\text{O}_3$  (d). All data are averaged by weighting over the AM1.5 solar spectrum in the 300-1100 nm spectral range. Note that the non-absorbed part (green) represents the light that exits the simulation box, i.e. it accounts both for light that does not interact with the NP and for light that is scattered by the NP. For c-Si (Fig. 3(a)), the graph shows that increasing the particle diameter from 5 to 60 nm drastically increases the absorption in the NP from 0 to 20%, due to the increased volume of the metal NP. On the other hand, the absorption in the c-Si (blue) is increased only from 12% to 14%. The maximum achievable absorption enhancement in the c-Si is limited by the large absorption in the metal NP. It must be concluded that the poorly absorbing indirect semiconductor Si can not be efficiently sensitized by Ag NPs. While the absorption in a very poorly absorbing Si slab can be enhanced (see Fig. 1) to make it slight less poor, full absorption in the Si as desired for photovoltaic applications cannot be achieved with Ag NPs.

Figure 3(b) shows that increasing the particle diameter in PF10TBT:PCBM significantly in-

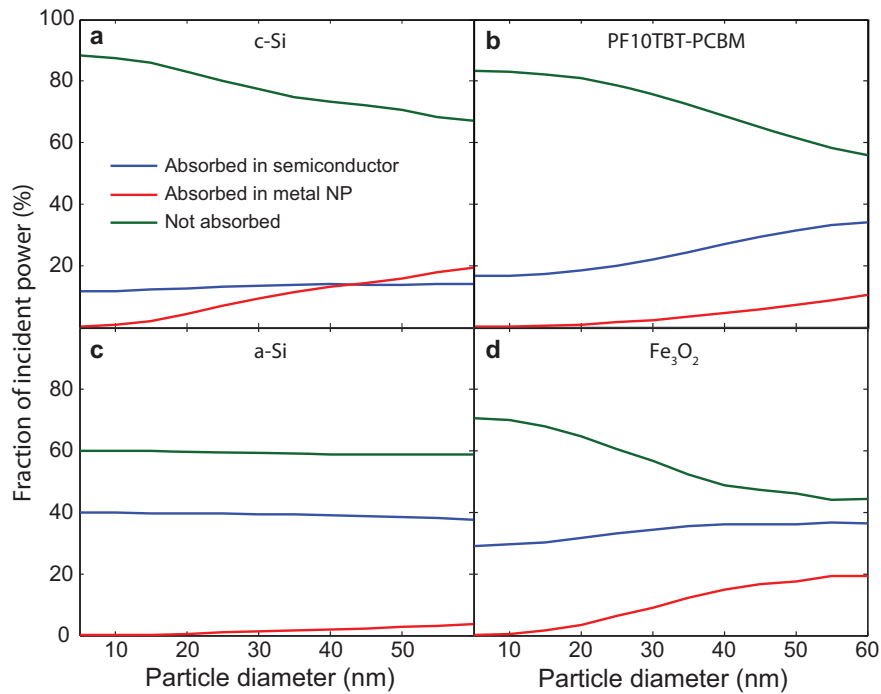


Fig. 3. Fraction of the incident power that is absorbed in the semiconductor (blue), in the metal NP (red) or not absorbed (green), as a function of particle diameter, for c-Si (a), PF10TBT:PCBM (b), a-Si (c) and Fe<sub>2</sub>O<sub>3</sub> (d). All data are averaged by weighting over the AM1.5 solar spectrum in the 300-1100 nm spectral range. The reduction of the non-absorbed power (green) is associated with an increase of the absorption in the substrate and in the NP. For the polymer substrate, the absorption in the active layer is larger than the losses in the metal. For a c-Si and Fe<sub>2</sub>O<sub>3</sub> substrates, the strong absorption in the NP strongly limits the plasmonic near-field absorption enhancement in the substrate. In an a-Si substrate no significant change is observed as a result of the resonant wavelength being larger than the bandgap wavelength.

increases the absorption in the polymer from 17% to 34% (see also Fig. 2(b)) while absorption in the NP increases from 0 to 10%. In this case the absorption in the semiconductor is thus significantly enhanced while absorption in the metal remains modest (compared to the case for c-Si). The data indicate, however, that increasing diameter the relative contribution of absorption in the metal increases. For larger particles scattering of light will also become dominant, due to the larger albedo, and a reduction of the near field absorption will occur.

Figure 3(c) shows the data for a-Si. A very small variation in both the absorbed and the non-absorbed fraction of incident power are observed as the particle diameter is increased from 5 to 60 nm, because the plasmon resonance occurs at a wavelength above the bandgap. The absorption in the metal NP (red) is relatively low (~3%) because a-Si is a strong absorber. For Fe<sub>2</sub>O<sub>3</sub> (Fig. 3(d)) a behavior similar to that for c-Si is observed. For large diameters a significant fraction of the light (20%) is absorbed in the NPs, while the absorption in the semiconductor is only slightly enhanced.

The analysis conducted so far shows the importance of matching the wavelength of the plasmon resonance with a spectral range where the hosting material is a good absorber. In particular, for materials like c-Si and a-Si, the large refractive index shifts the resonance to larger

wavelengths where these materials are poorly absorbing. One possible way to shift the plasmon resonance to shorter wavelengths is to coat the NP with a thin dielectric layer (core-shell particle). The presence of such a dielectric shell can also serve, in a photovoltaic device, as an electrical passivation of the metal surface to avoid carrier recombination at the NP interface.

We have simulated the absorption cross-section spectra for core-shell Ag-SiO<sub>2</sub> particles embedded in a c-Si substrate (see inset in Fig. 4(b)). The core particle diameter is 30 nm, and the shell thickness is varied between 0 and 5 nm. Figure 4(a) shows the LSPR resonance wavelength as a function of the shell thickness. A strong blue shift is observed as the shell thickness increases, as expected due to the reduced refractive index in the plasmonic near field. Figure 4(a) (top axis) also shows the absorption coefficient of c-Si as function of wavelength. The graph shows that increasing the shell thickness to 5 nm shifts the resonance to a spectral range where the c-Si is more strongly absorbing. Figure 4(b) shows the absorption enhancement in

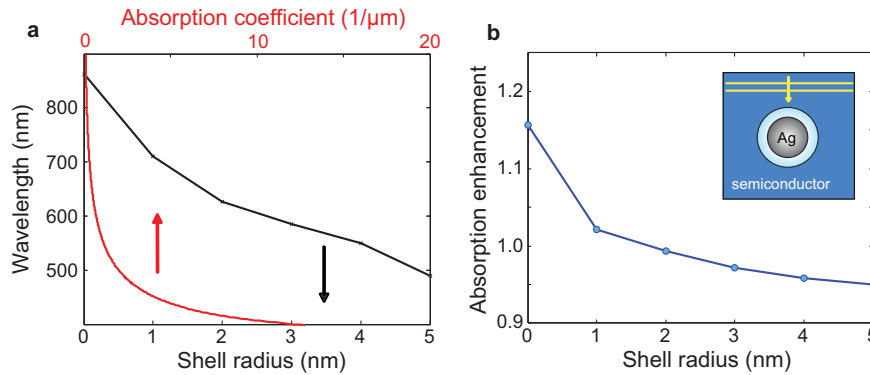


Fig. 4. (a) LSPR dipolar resonance wavelength (black line, vertical axis) as a function of the shell thickness (bottom axis), for a Ag/SiO<sub>2</sub> core-shell particle embedded in a c-Si layer. The Ag core diameter is 30 nm. A strong blue shift is observed as the silica shell thickness increases. Also shown is the absorption coefficient of c-Si (red line, top axis) as a function of wavelength. Increasing the shell thickness shifts the resonance into a spectral range where Si is more absorbing. (b) Absorption enhancement, averaged by weighting over the AM1.5 solar spectrum in the 300-1100 nm spectral range, in the c-Si substrate as a function of the shell thickness. A reduction in absorption is observed for larger shell thicknesses as a result of the reduced overlap of the near-field with the active material.

the c-Si substrate as a function of the shell thickness, again integrated over the AM1.5 solar spectrum from 300-1100 nm. The graph shows a clear reduction of the absorption enhancement as the shell thickness increases. Despite the fact that the dipole resonance is shifted into a spectral range where c-Si is more absorbing, the fraction of the near-field that overlaps with the c-Si substrate is reduced due to the presence of the dielectric layer around the particle. The net effect is a reduction of the absorption in the semiconductor layer. Similar results were found for all other semiconductors shown in Figs. 2 and 3. The use of a dielectric shell to tune the LSPR is thus not an effective way to enhance the absorption in the semiconductor.

An alternative way to tune the NP plasmonic resonance is by changing its shape. Figure 5 shows the average absorption, integrated over the AM1.5 solar spectrum for prolate (crosses) and oblate (circles) Ag spheroids with size aspect ratios ranging from 0.1-1.0. Data are shown for a spheroidal NP embedded in c-Si (a) and PF10TBT:PCBM (b). The particle volume for the spheroids is kept equal to that of a 30-nm-diameter sphere. Absorption in the semiconductor (blue) and in the Ag NP (red) is shown as a function of the size aspect ratio (short over long axis length) of the spheroid. The data for size aspect ratio 1 (i.e. spheres) equals that in the

corresponding panels of Fig. 3. The absorption in a semiconductor volume without the NP is shown for reference in Fig. 5 (dashed black line). For the case of c-Si (Fig. 5(a)), changing the

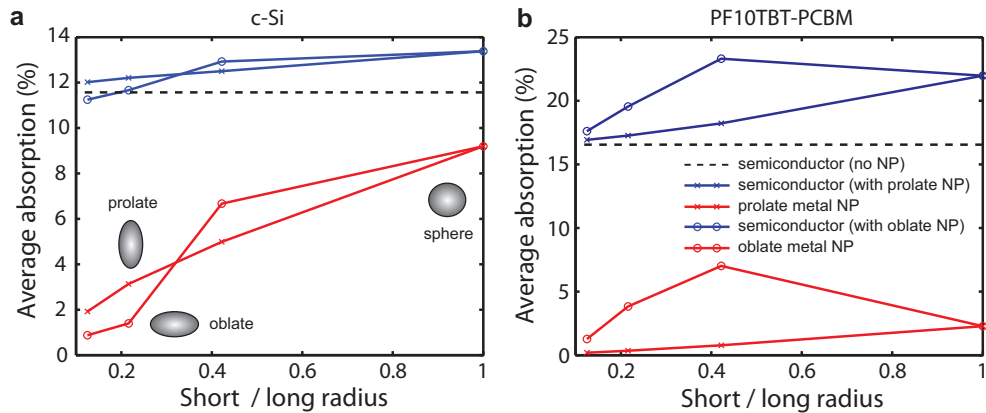


Fig. 5. AM1.5 averaged absorption in c-Si (a) and PF10TBT:PCBM (b) for oblate (circles) and prolate (crosses) embedded Ag nanoparticles. Absorption in the semiconductor (blue) and in the metal NP (red) is shown as a function of the ratio of the short radius over the long radius of the spheroid. The absorption of a bare semiconductor volume is shown for reference (dashed black line). The graph shows that an increase in the absorption in the semiconductor due to the presence of the NP is always associated with strong Ohmic losses in the metal NP.

particle shape from spherical to spheroidal leads to a reduction of the absorption in c-Si for all aspect ratios. This is due to a reduced near-field intensity for prolate spheroids, and the redshift of the plasmonic resonance in the case of oblate spheroids. For the case of PF10TBT:PCBM (5(b)), the absorption in the polymer for an oblate spheroid with a ratio of short over long radius of about 0.4 (23.7%) is slightly larger than the case of a spherical particle (22%). However, this increase is accompanied by an even higher increase of Ohmic losses in the metal NP (from 2% in a sphere to 7% in an oblate spheroid). For prolate NPs a reduction of the absorption in the polymer semiconductor is observed for all aspect ratios, compared to spherical NPs. Overall, Fig. 5 shows that also for spheroidal particles absorption enhancement in the semiconductor can only be achieved at the expenses of strong Ohmic losses in the metal.

So far only the absorption of the local field around a single NP in a single 100-nm-box has been considered. In order to extend our study to a realistic planar device geometry, we consider square arrays of Ag NPs embedded in a 100-nm-thick semiconductor layer, infinitely extended in the two in-plane directions by using Periodic Boundary Conditions (PBCs). Figure 6 shows the average absorption, weighed over the AM1.5 solar spectrum, for arrays of silver NPs embedded in a c-Si (a) and PF10TBT:PCBM (b) layer. In each panel, the absorption in the hosting material (blue lines) and in the metal NPs (red lines) is shown as a function of the ratio of the array pitch over the particle diameter, for particles with 5 nm (dash-dotted lines) or 40 nm (dashed lines) diameter. The absorption in a substrate without NPs is shown for reference (black solid line). Figure 6(a) shows that for c-Si the highest absorption (13%) can be achieved for the smallest array pitch (i.e. equal to 1.5 times the NP diameter), a result that is in agreement with the previous work by Vedraïne *et al.* [19, 34]. This can be explained by a stronger overall interaction of the NPs with the incident light when they are packed closer together. Despite the absorption increases with respect to a layer without nanoparticles (black line, 9.6%), it must be noted that for such configurations the absorption in the metal NP due to ohmic losses is also significantly increased, up to a value of 14% (i.e. higher than the absorption in the c-Si). The

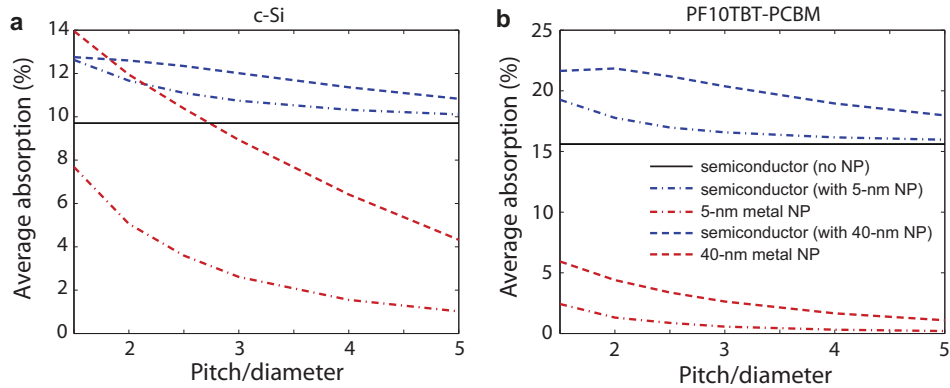


Fig. 6. Average absorption for arrays of silver NPs embedded in a c-Si (a) and PF10TBT:PCBM (b) substrate. Data are plotted for particles with 5 nm (dash-dotted lines) and 40 nm (dashed lines) diameter, as a function of the ratio of the array pitch over the particle diameter. Absorption in the hosting material is shown in blue, absorption in the metal NPs is shown in red. The absorption in a substrate without NPs is shown for reference (black solid line). For both c-Si and PF10TBT:PCBM, the highest absorption in the semiconductor is achieved for NP arrays with short inter-particle distance compared to the NP size. In the case of c-Si (a), the increase in absorption in the c-Si layer comes at the expense of a significant increase in the ohmic losses in the metal NPs.

large ohmic losses are a direct consequence of the higher density of metal NPs in the layer. Once again, we must conclude that c-Si cannot be efficiently sensitized by Ag NPs.

Figure 6(b) shows a similar graph for a PF10TBT:PCBM layer. In this case, the largest absorption is obtained for arrays with a pitch equal to 1.5 and 2 times the NP diameter, for 5-nm- and 40-nm-diameter particles respectively. The absorption of a layer without NPs (16%) is increased to 22% for an array of 40-nm-diameter NPs with 80 nm pitch. Similar to the case of c-Si, the increase in absorption in the polymer layer always comes at the expense of increased ohmic losses in the metal.

Finally, we study the dependence of absorption in a semiconductor with embedded Ag NPs on the thickness of the semiconductor layer. We consider a square array of 40-nm-diameter Ag NPs, spaced by 100 nm, and placed 40 nm below the semiconductor surface. A sketch of the simulation geometry is shown in Fig. 7(a). The NP array is placed 40 nm below the surface of the semiconductor. As a first step, we calculate the absorption profiles as a function of depth. Figure 7(b) shows the absorptance per unit length (top axis) as a function of depth (right axis) for a bare c-Si substrate (black), in a c-Si substrate with embedded Ag NPs (blue) and in the Ag NP array (red). The graph shows that, in the proximity of the NPs (i.e. for depths smaller than 80 nm), the absorption in the c-Si is enhanced by the presence of the NP due to the strong plasmonic near field (see also Fig. 1(a)). Similarly to Fig. 1(a), the absorption in the c-Si with the NP is limited by the large absorption in the metal (red line). Absorption in the Ag particles is 2 to 3 times stronger than in the c-Si. In the region beyond the NPs (i.e. for depths larger than 80 nm), the absorption of the c-Si with the NPs is slightly lower than that of the bare c-Si substrate, due to the fact that more light is absorbed in the top layer (either in the semiconductor or in the metal). A similar qualitative behavior is observed for Ag NPs embedded in a PF10TBT:PCBM layer (Fig. 7(c)). In this case however, a significant absorption enhancement is observed for the polymer containing the NP array (blue) with respect to the bare polymer (black), in the proximity of the NP array. The absorption in the NPs (red) is less than one third of the absorption in the polymer, similarly to what was shown in Fig. 1(b). In the

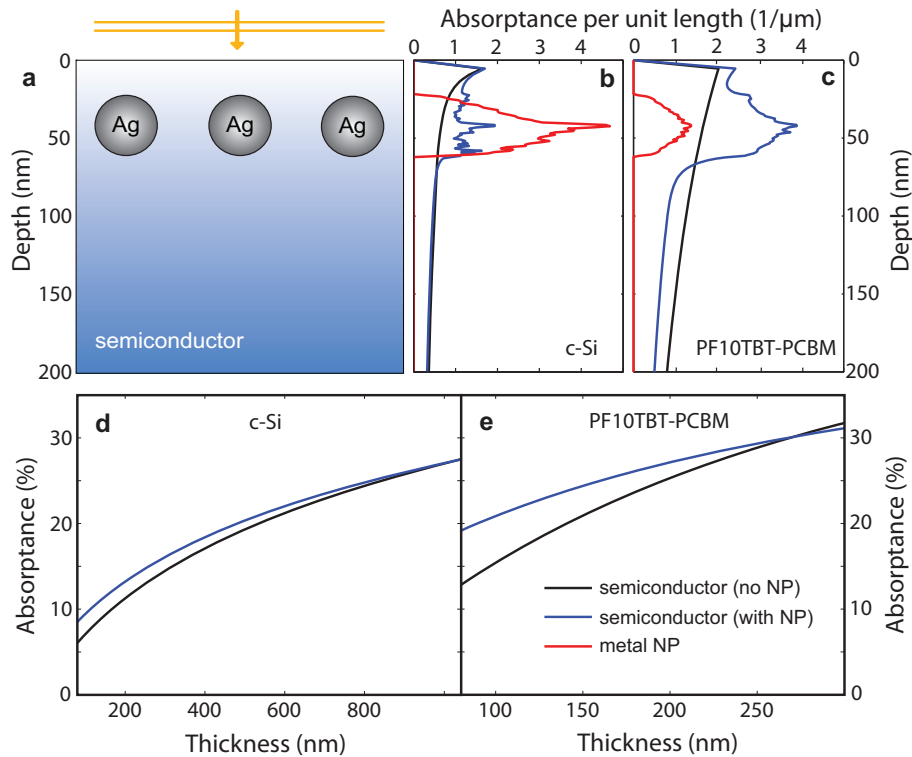


Fig. 7. (a) Sketch of the simulation geometry. A square array of 40-nm-diameter Ag NPs, spaced by 100 nm, is placed 40 nm below the surface of a semi-infinite semiconductor layer. (b, c) Absorbance per unit length (top axis) as a function of depth (right axis) for a bare substrate (black), in a substrate with embedded Ag NPs (blue) and in the Ag NP array (red), for c-Si (b) and PF10TBT:PCBM (c). Absorption in the active layer is enhanced by the presence of the NP in the proximity of the NP, due to the strong plasmonic near field. (d, e) Absorbance in a bare substrate (black) and in a substrate containing a Ag NP array (blue), for a c-Si (d) and PF10TBT:PCBM (e) substrates, as a function of layer thickness. For thinner layers, absorption is enhanced by the LSPR near field of the NP. For thicker layer, the bare substrate shows larger absorption than a substrate with NPs, as a result of the metal losses in the latter.

region beyond the NP array, the absorption in the bare polymer substrate is higher than that of the polymer containing the NP array, due to the stronger absorption in the near-field region.

The data shown in Figs. 7(b) and 7(c) can be used to calculate the absorptance for layers of different thicknesses, by integrating the absorptance per unit length over the depth, according to:  $A(t) = \int_0^t a(x)dx$ , where  $a$  is the absorptance per unit length at the depth  $x$ ,  $t$  is the thickness and  $A$  is the absorptance. Figure 7(d) shows the absorptance as a function of layer thickness for a bare c-Si substrate (black) and a c-Si substrate containing the NP array (blue). For layers thinner than 1 micron, the absorptance is enhanced by the presence of the NP array. This is due to the fact that the bare layer is poorly absorbing and the absorptance is enhanced by the strong near field of the particle. For a layer of 1 micron, however, the absorption of the bare layer is equal to the absorption in the layer containing the NP. In fact, in the limit of very thick layers (not shown here), the bare c-Si fully absorbs the light transmitted in the layer, but the absorption in the layer with the NPs is limited by the metal losses. Thus the two curves cross at a thickness of about 1 micron. The same behavior is observed for PF10TBT:PCBM (Fig. 7(e)). In this case, a significant absorption enhancement is observed for layer thicknesses below 200 nm. For example, the absorptance of a 100 nm thick layer increases from 15% to 21% due to the presence of the NP array. We note that the same absorptance is achievable with a 170 nm layer of bare polymer, and thus the NP array allows reducing the layer thickness by 40% for the same absorption. This is advantageous given the very low carrier diffusion length in the polymer (order of 10 nm), which limits the thickness of a photovoltaic device to less than 100 nm.

### 3. Discussion and conclusion

Metal NPs embedded in a semiconductor material enhance light absorption in the semiconductor, due to the plasmonic near-field enhancement. The absorption enhancement occurs at wavelengths close to the LSPR of the metal NP, which depends on particle size, shape, inter-particle spacing and on the refractive index and thickness of the embedding layer. In all studied geometries and semiconductor materials, strong unwanted absorption occurs by Ohmic dissipation in the metal NPs. For a poorly absorbing semiconductor such as c-Si, Ohmic dissipation in the metal is the dominant loss mechanism. In fact, in c-Si only a small (20%) absorption enhancement is observed at the expense of large absorption losses in the metal. We conclude it is not practical to sensitize c-Si with Ag NPs. For a 100-nm thick PF10TBT:PCBM layer, the total absorbance, integrated over the solar spectrum from 300-1100 nm, is enhanced from 17 to 34%. For thicker layers or higher NP concentrations, the ultimate absorbance that can be achieved is limited by the Ohmic dissipation in the metal (10%, see Fig. 3(b)), which constitutes about one quarter of the total absorbance for large NPs (44%, metal + semiconductor). Similarly, an absorption enhancement up to only 24% is found for Fe<sub>2</sub>O<sub>3</sub> layers. Here too, about one third of the total absorbance (57%, metal + semiconductor) in the NP-doped layer is due to Ohmic losses in the metal (20%). No absorption enhancement was found for a particle embedded in a-Si, due to the fact that the LSPR wavelength is larger than the bandgap wavelength of a-Si. We found that the use of core-shell particles, in order to shift the LSPR resonance in a spectral range where absorption is larger, is ineffective, due to the reduced overlap of the near-field with the active material. Similarly, the use of spheroidal particle is ineffective due to the reduced near-field intensity for spheroids with respect to spheres.

The strong near-field absorption enhancement can be used to reduce the thickness of a thin-film solar cell without a reduction of optical absorption. This is particularly useful for photovoltaic material, such as the polymer considered in this work, where the short carrier diffusion length limits the thickness of the cell. We have shown that the layer thickness of a polymer solar cell can be reduced from 170 to 100 nm by adding Ag NPs. Nonetheless, it must be stressed that

none of the NP-sensitized geometries enable to achieve full absorbance in the semiconductor.

Finally, we note that in this work the effect of light scattering have been only marginally considered. Further studies are required to investigate the possible benefits of scattering on light absorption in the active layer.

### **Acknowledgments**

We thank SARA Computing and Networking Services ([www.sara.nl](http://www.sara.nl)) for their support in using the Lisa Compute Cluster. This work is part of the research program of the Foundation for Fundamental Research on Matter (FOM) which is financially supported by the Netherlands Organization for Fundamental Research (NWO). It is also funded by the European Research Council (ERC). This work is also part of the Global Climate and Energy Project (GCEP).